Proceedings of the Korean Nuclear Society Autumn Meeting
Taejon, Korea, October 2000

Cuntercurrent Flooding Critical Heat Flux under Zero Flow conditions in Vertical Annulus with Uniformly and Non-uniformly Heated Sections

Se-Young Chun, Sang-Ki Moon and Sun-Kyu Yang

Korea Atomic Energy Research Institute
150 Dukjin-dong, Yusong-gu, Taejon, 305-353, Korea

Abstract

The experimental study of water CHF (critical heat flux) under zero flow conditions were carried out in an annulus flow channel with uniformly and non-uniformly heated sections over a pressure range of 0.52 to 14.96 MPa. A comparison of the present data with the existing flooding CHF correlations shows that the predicted values by the existing flooding CHF correlations give considerably lower values than the present data. When the correction terms with the density ratio and the effect of the heat flux distribution proposed in the present work are used with the CHF correlation based on the Wallis flooding correlation, it predicts the measured flooding CHF within an RMS error of 9.0 %.

1. Introduction

Correct characterization of the critical heat flux (CHF) is of particular interest when predicting nuclear reactor core behavior for accident situations, including a flow transient such as reactor circulation pump failure and a loss of coolant accident (LOCA). The core coolant flow is reduced during a large portion of several types of accident scenarios, and the reactor core encounters a stagnant or reverse flow. The understanding of the fundamental nature of CHF in the vertical flow channel under stagnant or zero flow condition will be important for reactor safety, as is the case with low flow CHF. In the case of a vertical channel with a larger liquid volume or shorter heated section, it may be inferred easily that the CHF mechanism becomes similar to the departure from nucleate boiling (DNB) in pool boiling. The CHF mechanism for a narrow and long vertical channel under a zero flow condition may be different from that of the pool boiling CHF.

Several investigators [1-4] have conducted experiments on CHF under very low flow conditions from several hundred kg/m^2s to a zero inlet flow with a completely closed bottom end. They have observed that a countercurrent flow is formed in the vertical flow channel at zero and very low flow rates, and subsequently the CHF occurs due to the countercurrent flow limitation (CCFL) or flooding. The CHF in these boiling systems was considerably smaller than that of normal pool boiling [2-3]. The experiments of El-Genk et al. [3] indicated that the CHF values with zero flow were about 30 % lower than those with net water upward flow when extrapolated to zero flow. For practical applications in the non-nuclear industry, many studies on the CHF phenomenon of the countercurrent flow of a heated vertical tube closed at the bottom end have been made with respect to the design and performance of closed two-phase thermosyphons. Flooding in the countercurrent flow was regarded and discussed by many investigators as one of the CHF mechanisms, and empirical flooding equations were employed in the development of the correlations for prediction of the CHF. Hence, the CHF of this sort is called the flooding CHF. The flooding CHF correlations were based on the Wallis empirical equation [5] obtained from the countercurrent flow in water and air two-phase system or the Kutateladze criterion for the onset of flooding, with the assumption of mass and energy balance.

The thermal hydraulics system codes most widely used for analyzing accidents in nuclear power plants are RELAP5/MOD3 and TRAC-PF1. In these codes, the Biasi correlation [6] and the AECL-UO CHF Look-up table [7], which are based on the data base of normal upward flow CHFs in tubes, are employed for the prediction of CHF. To provide the CHF value for the zero flow conditions, the Biasi correlation is evaluated at a mass flux of 200 kg/m^2s and the CHF Look-up table uses the Zuber

pool boiling CHF correlation [8] with a void fraction correction suggested by Griffith et al. [9]. It is obvious that the codes adopt inappropriate methods to predict the CHF under zero flow conditions. The experimental studies of the CHF in closed two-phase thermosyphons have been made using a uniformly heated vertical tube without a liquid reservoir at the top of the heated section. The conditions of the nuclear reactor may require the vertical test channel with the non-uniformly heated section and the liquid reservoir.

In the above references, the CHF experiments were carried out under near atmospheric pressure conditions. The authors have conducted the CHF experiments for zero inlet flow in uniformly and non-uniformly heated vertical annuli with a liquid reservoir under high pressure conditions [10,11]. In this paper, several existing correlations for the countercurrent flooding CHF are compared with the CHF data obtained in the previous experiments to examine the applicability of the correlations.

2. Experiments

A description of the facility, the experimental procedure and results can be found in references [10-12]. A brief description will be presented here in order to orient the reader.

Figure 1 shows the details of the test section used in the present experiments. The test section consists of a vertical annulus flow channel and upper and lower plenums. The upper plenum is connected to a steam/water separator. As shown in Fig. 2, in the heater rod with non-uniform axial power, the power level is divided into 10 steps with a minimum and maximum power ratio of 0.448 and 1.400, respectively, to simulate a symmetric chopped cosine heat flux profile.

The CHF experiments have been performed by the following procedure. First, the circulation pump, preheater and pressurizer are operated for raising the temperature of the loop and establishing inlet subcooling and pressure of the test section at the desired levels, and the isolation valve located at the upper stream of test section is fully closed. Power is applied to the heater rod of the test section and increased gradually in small steps up to the CHF occurrence. The period between the power steps is chosen to be sufficiently long (about fifteen minuets) so that the loop could stabilize at the steady-state conditions.

In the present experimental conditions, the water temperature (T/CW 2) at the bottom end of the heated section remained in a subcooled condition during a run of the experiment, in spite of the fact that power was applied to the heater rod and the water of the heated section was being heated. This is due to the existence of relatively large heat loss and convective heat transfer toward the lower plenum in the present test section arrangement. A total of 135 CHF data were obtained in the ranges of the water subcooling enthalpies from 85 to 413 kJ/kg at the bottom end of the heated section and system pressures from 0.52 to 14.96 MPa. The pressure at the top end of the heated section is specified as the system pressure and is used for the analysis of the experimental data.

3. Data Reduction

In the flooding phenomenon for countercurrent flow, the vapor flow rate is the most important parameter. As mentioned above, the water at the bottom part of the heated section is under a subcooled condition at the occurrence of a CHF. In this situation, the amount of steam generated in the heated section cannot be evaluated directly from the mass and energy balances. The information for the locations of the onset of saturated boiling is required to evaluated the vapor flow rate at the top end of the heated section.

We can consider a countercurrent annular flow as illustrated in Fig. 3. In order to search for the locations of the onset of saturated boiling in the present boiling system, it is assumed that the pressure losses due to friction and acceleration can be neglected for the pressure difference DP between the bottom end of the heated section (Z=0) and location Z, and that the void fraction in the subcool boiling region is negligibly small. The pressure difference DP is equal to the static head from the bottom end of the heated section to location Z. Consequently, the average void fraction α from the bottom end (Z=0) to location Z is given as

$$a = \frac{r_{l,sat} gZ + (r_{l,sub} - r_{l,sat}) gZ_{sat} - \Delta P}{(r_g - r_{l,sat}) g(Z - Z_{sat})}, \quad (1)$$

where r_l and r_g are the liquid and vapor densities, and g is the gravitational acceleration. The subscripts *sub* and *sat* denote the subcooling and saturation conditions, respectively.

For the present test section, the pressure difference $DP_{m\text{-}2}$ measured by the differential pressure transmitter DP-2 (see Fig. 1) are plotted as a function of subcooling temperature DT_{sub} at the bottom end of the heated section for a given system pressure in Fig. 4. In the present conditions, it was observed that the relationship between $DP_{m\text{-}2}$ and ΔT_{sub} is linear for a fixed system pressure. The pressure difference $DP_{m\text{-}2,sat}$ for DT_{sub}= 0 (i.e., Z_{sat}= 0) at the bottom end of the heated section can be given from the extrapolation of the liner relationship between $DP_{m\text{-}2}$ and DT_{sub}. Substituting the values of $DP_{m\text{-}2,sat}$, Z (in the present case, Z = 1.042 m) and Z_{sat}= 0 into Eq. (1), the average void fraction a_o for the saturated condition at the bottom end of the heated section is calculated for each system pressure. When it is assumed that a decreases linearly in proportion to the increase of distance Z_{sat} from the bottom end of the heated section to the saturation point, the void fraction a is expressed as follows:

$$a = a_o \left(1 - \frac{Z_{sat}}{Z}\right). \quad (2)$$

Location Z_{sat} of the onset of saturated boiling is given from Eqs. (1), (2) and the measured pressure difference $DP_{m\text{-}2}$. For calculating Eq. (1), the subcooled liquid density $r_{l,sub}$ in the bottom region of the heated section uses that for an average of the temperature at the bottom end of the heated section and the saturated temperature.

Subsequently, the boiling length L_B at CHF conditions is defined using the heated length L_h as follows:

$$L_B = L_h - Z_{sat}. \quad (3)$$

The average CHF $q_{C,B}$ over the boiling length is expressed by

$$q_{C,B} = \frac{1}{L_B} \int_{Zsat}^{L_h} q(z) dz, \quad (4)$$

where $q(z)$ are the axial heat flux profile of the heater rod. In the present work, the experimental data are analyzed with the boiling length L_B and the average CHF q_{CB}.

4. Comparison of the Experimental Data with Existing correlations for flooding CHF

4.1. Existing correlations

The empirical flooding correlations have been useful to estimate the CHF in a heated vertical channel closed at the bottom end. One of the most frequently used correlations for flooding was given by Wallis [5], in the following expression:

$$j_g^{*1/2} + m j_l^{*1/2} = C_w, \quad (5)$$

where j_g^* and j_l^* are the dimensionless superficial velocities of vapor and liquid, respectively, and C_w is a constant, mainly depending upon the tube end conditions. C_w has values from 0.725 to 1.0, from the flooding experimental results in the countercurrent flow. The constant m is set to unity in the conditions of the present work. The dimensionless superficial velocities j_g^* and j_l^* are defined by

$$j_g^* = j_g r_g^{1/2} (gD\Delta r)^{-1/2} \quad (6)$$

$$j_l^* = j_l r_l^{1/2} (gD\Delta r)^{-1/2}, \quad (7)$$

where j_g and j_l are the superficial velocities of gas and liquid, respectively, D is the inner diameter of the tube, and Dr is the density difference (r_l - r_g) between the liquid and vapor phases. For the boiling system shown in Fig. 3, when the heated area A_B over the boiling length is employed, the following mass and energy balance equation holds under steady-state conditions:

$$j_g r_g A_f = j_l r_l A_f = \frac{q_{C,B} A_B}{h_{lg}}, \tag{8}$$

where A_f is the flow area of the channel, and h_{lg} is the latent heat of vaporization. Substituting Eq. (8) into Eq. (5) and using a hydraulic equivalent diameter D_{hy} in Eqs. (6) and (7) for the annulus channel, the CHF due to flooding is expressed in a dimensionless form as in the following equation:

$$\frac{q_{C,B}}{h_{lg}(gD_{hy} r_g \Delta r)^{1/2}} = \frac{C_w^{\,2}}{4}\left(\frac{D_{he}}{L_B}\right)\left[1+\left(\frac{r_g}{r_l}\right)^{1/4}\right]^{-2}. \tag{9}$$

In the above equation, the heated equivalent diameter to the boiling length ratio $D_{he}/(4L_B)$ was used instead of the term A_f/A_B. The CHF $q_{C,B}$ and the boiling length L_B are calculated from Eqs. (4) and (3), respectively. Sakhuja [13] showed that Eq. (9) agreed with his experimental data for tubes.

Mishima and Nishihara [2] rewrote Eq. (9) as follows:

$$\frac{q_{C,B}}{h_{lg}(g l r_g \Delta r)^{1/2}} = \frac{C_w^{\,2}}{4}\left(\frac{D_{he}}{L_B}\right) D^{*1/2}\left[1+\left(\frac{r_g}{r_l}\right)^{1/4}\right]^{-2}, \tag{10}$$

where D^* is the dimensionless diameter, defined by $D^*=D_{hy}/l$. The length scale l of the Taylor instability is given by $l = (s/gDr)^{1/2}$, where s is the surface tension. Therefore, D^* used by Mishima and Nishihara is equal to the Bond number, $B_o = D_{hy}(gDr/s)^{1/2}$. They reported that the flooding CHF was well reproduced by Eq. (10) with $C_w^{\,2} = 0.96$ for an annulus.

Nejat [14] proposed a flooding CHF correlation based on Eq. (9). The original form of the Nejat correlation for the tube is as follows:

$$\frac{q_{C,ax}}{h_{lg} r_g (gD)^{1/2}}\left(\frac{L_B}{D}\right)^{-0.1} = C_w^{\,2}\left(\frac{\Delta r}{r_g}\right)^{1/2}\left[1+\left(\frac{r_g}{r_l}\right)^{1/4}\right]^{-2}. \tag{11}$$

where $q_{C,ax}$ is the CHF in an axial direction, defined by

$$q_{C,ax} = \frac{pD}{A_f}\int_{Zsat}^{L_h} q(z)\,dz.$$

Nejat added the correction term $(L_B/D)^{-0.1}$ in the correlation in order to reduce the scatter of the experimental data points on the tubes, and then showed that Eq. (11) with $C_w^{\,2} = 0.36$ satisfactorily correlates the experimental data. Using the CHF q_{CB} in the heated surface and the heated equivalent diameter D_{he} in the correction term, Eq. (11) is rewritten as

$$\frac{q_{C,B}}{h_{lg} r_g (gD_{hy})^{1/2}} = \frac{C_w^{\,2}}{4}\left(\frac{D_{he}}{L_B}\right)\left(\frac{\Delta r}{r_g}\right)^{1/2}\left[1+\left(\frac{r_g}{r_l}\right)^{1/4}\right]^{-2}, \tag{12}$$

where $C_w^{\,2}$ is $0.36(L_B/D_{he})^{0.1}$.

Several investigators have employed Kutateladze's criterion for the onset of flooding, given by the following expression:

$$K_g^{\,1/2} + mK_l^{\,1/2} = C_k \tag{13}$$

where K_g and K_l are defined by $K_g = j_g r_g^{1/2}(g\,sDr)^{-1/4}$ and $K_l = j_l r_l^{1/2}(g\,sDr)^{-1/4}$, respectively, and C_k is a constant. Pushkina and Sorokin gave $m = 0$, $C_k^2 = 3.2$ for the flooding condition [15]. Substituting j_g and j_l into Eq. (13) and setting the value of m to unity, a correlation for the flooding CHF is given by the following expression:

$$\frac{q_{C,B}}{h_{lg}(g s r_g^{\,2}\Delta r)^{1/4}} = \frac{C_k^{\,2}}{4}\left(\frac{D_{he}}{L_B}\right)\left[1+\left(\frac{r_g}{r_l}\right)^{1/4}\right]^{-2}. \tag{14}$$

Tien and Chung [16] gave the form of C_k including a correction term with a function of the Bond number B_o as follows: $C_k^2=3.2[\tanh(B_o^{1/4}/2)]^2$.

The empirical correlation with a similar form to Eq. (14) was derived by Imura et al. [17]. The correlation is expressed by

$$\frac{q_{C,B}}{h_{lg}(g s r_g^{\,2}\Delta r)^{1/4}} = \frac{C_k^{\,2}}{4}\left(\frac{D_{he}}{L_B}\right)\left(\frac{r_g}{r_l}\right)^{-0.13}. \tag{15}$$

Imura et al. reported that Eq. (15) with $C_k^2 = 0.64$ correlated the experimental data within ± 30 % accuracy.

Mishima and Nishihara [2] reported that the flooding CHF is correlated using Eq. (10) with C_w = 1.66, 0.98 and 0.73 for tubes, annuli and rectangular channels, respectively. In Nejat's Eq. (11), C_w was modified with the term of L_B/D, and Tien and Chung proposed Eq. (14) with a correction term relating to the Bond number B_o for C_k. This implies that the values of C_w and C_k are not constant and vary with the geometry and thermodynamic conditions. Equations (9) and (14) show that the flooding CHF is a function of L_B/D_{he}, B_o and r_g/r_l. Park et al. [18] examined the effects of the terms L_B/D_{he}, B_o and r_g/r_l on C_w^2 using Eq. (9) based on the Wallis flooding equation and proposed the empirical correlation for C_w^2 as follows:

$$C_w^{\,2} = 1.22\left(\frac{L_B}{D_{he}}\right)^{0.12}\left(\frac{r_g}{r_l}\right)^{0.064}(1+0.055B_o-4.08\times10^{-3}B_o^{\,2}). \tag{16}$$

They reported that the flooding CHF is predicted within a RMS (root mean square) error of 18.8 % when Eq. (16) for C_w^2 is used with Eq. (9).

4.2. Comparison with existing correlations

The present data are compared with Eqs. (10), (12), (14) and (15), using the dimensionless parameters as follows:

$$q^*_{C,w} = \frac{q_{C,B}}{h_{lg}(gD_{hy}r_g\Delta r)^{1/2}}, \qquad q^*_{C,N} = \frac{q_{C,B}}{h_{lg}r_g(gD_{hy})^{1/2}}, \qquad q^*_{C,k} = \frac{q_{C,B}}{h_{lg}(g s r_g^{\,2}\Delta r)^{1/4}} \quad \text{and}$$

$$x = \left[1+\left(r_g/r_l\right)^{1/4}\right]^{-2}.$$

The results of the comparison are shown in Figs. 5~8. Figures 5, 7 and 8 show that Eqs. (10), (14) and (15) greatly depend on the axial heat flux distribution of the heated section. In Fig. 5 for the Mishima and Nishihara equation, the experimental data points have a large scatter in both heat flux distributions. The Kutateladze flooding CHF correlation (Eq. (14)) and Imura et al.'s correlation (Eq. (15)) reasonably correlate the experimental data for the uniform heat flux, but the experimental data for the non-uniform heat flux are considerably scattered as shown in Figs. 7 and 8. On the other hand, Fig. 6 shows that the Nejat equation (12) better correlates the experimental data in the range of pressures from 3.02 to 14.96 MPa. The discrepancy between the uniform and non-uniform heat fluxes tends to become large as the pressure decreases, particularly in the low pressure region (from 0.52 to 1.79

MPa). When C_w^2 and C_k^2 suggested by each investigator are used, the dimensionless parameters q_C^* calculated by Eqs. (10), (12), (14) and (15) give considerably lower values than the present data. In the comparison with Eq. (14), the value of 3.2 is used as C_k^2, because the use of the Bond number term of Tien and Chung produces a large difference between the present data and the calculated values. The form of the Bond number term of Tien and Chung may not be appropriate.

Equations (10), (12) and the Park et al. correlation for C_w^2 were derived using Eq. (9) based on the Wallis flooding equation. When C_k^2 in Eq. (14) is set to $3.2C_w^2$ and Eq. (16) for C_w^2 is used, Equation (14) essentially has the same form as Eq. (10) because Eq. (16) includes the Bond number term. The original correlation of Imura et al. [17] was derived independently of the flooding correlation. The density ratio $(r_g/r_l)^{-0.13}$ and the constant value of 0.64 for C_k^2 in the right-hand side of Eq. (15) were determined empirically from their experimental results that the effect of B_o on the CHF is not recognized at a constant r_g/r_l condition. Katto and Hirano [19] pointed out that the right-hand side of Eq. (15) is nearly equivalent to the right-hand side of Eq. (9) except for the value of C_w^2. Therefore, Park et al.'s C_w^2 can be applied for Eqs. (10), (12), (14) and (15). As shown in Figs. 5 and 6, the values calculated by Eqs. (10) and (12) with C_w^2 of Park et al. draw tolerably toward the present data. Equation (10) with Park et al.'s C_w^2 gives a large scattering of the calculated $q_{C,k}^*$. Figures 7 and 8 show that the parameter $q_{C,k}^*$ calculated by Eqs. (14) and (15) with Park et al.'s C_w^2 appear in a region between the data points for uniform and non-uniform heat fluxes. The use of Park et al.'s C_w^2 in the flooding CHF equations yields better agreement than C_w^2 and C_k^2 suggested by each investigator. However, the discrepancy due to the effect of the heat flux distribution cannot be improved. As can be seen from Fig. 6, the present data are linearly correlated with Nejat's Eq. (12) and the parameter $q_{C,N}^*$ calculated using Park et al.'s C_w^2 do not scatter, although the effect of the heat flux distribution is large in the low pressure region.

The range of r_g/r_l used in the development of Imura et al.'s correlation covers the present experimental conditions. This means that the influence of the functional form of the density ratio term is large. The comparison of the ranges of the present conditions and the experimental data used by Park et al. [18] is listed in Table 1. In the range of the experimental data used in the development of Park et al.'s C_w^2, the density ratio r_g/r_l does not cover the present experimental conditions. Therefore, the term $(r_g/r_l)^{0.064}$ in Eq. (16) should be reformed as corresponds to the present conditions. In Eq. (9), the variation of C_w^2 $(= 4q^*_{C,w}L_B/(D_{he}x)$ for r_g/r_l can be obtained for the present data, and then, from the best fitting of the relation between C_w^2 and r_g/r_l, the functional form of r_g/r_l in Eq. (16) is obtained. As a result, the Park et al. correlation is rewritten as follows:

$$C_w^2 = 1.22\left(\frac{L_B}{D_{he}}\right)^{0.12}\left(\frac{r_g}{r_l}\right)^{-0.032}(1+0.055B_o-4.08\times10^{-3}B_o^2) \tag{17}$$

In order to take into account the effect of the heat flux distribution on the CHF, the length $L_{C,B}$ from the location of the onset of saturated boiling to the location of the CHF occurrence is introduced. Using Eq. (17) for C_w^2 and the ratio $D_{he}/L_{C,B}$ instead of the term D_{he}/L_B in Eqs. (9) and (14), and then plotting the terms $4q^*_{C,w}[1+(r_g/r_l)^{1/4}]^2/C_w^2$ and $4q^*_{C,k}[1+(r_g/r_l)^{1/4}]^2/C_w^2$ as a function of $D_{he}/L_{C,B}$, respectively, the functional forms of $D_{he}/L_{C,B}$ for the present data are determined as follows:

$4(D_{he}/L_{C,B})^{1.396}$ for Eq. (9) based on the Wallis flooding equation, and
$4(D_{he}/L_{C,B})^{1.160}$ for Eq. (14) based on the Kutateladze flooding criterion.

Equations (9) and (14) including the above terms give the results as shown in Figs. 9 and 10. These figures indicate that a pertinent use of the term $D_{he}/L_{C,B}$ can reduce the effect of the heat flux distribution on the CHF. In particular, Equation (9) with $(D_{he}/L_{C,B})^{1.396}$ is scarcely influenced by the heat flux distribution. Consequently, Equation (9) based on the Wallis flooding equation is rewritten as the following expression:

$$q_{C,B} = C_w^2\left(\frac{D_{he}}{L_{C,B}}\right)^{1.396} h_{lg}(gD_{hy}r_g\Delta r)^{1/2}\left[1+\left(\frac{r_g}{r_l}\right)^{1/4}\right]^{-2}, \tag{18}$$

where C_w^2 uses Eq. (17). In Fig. 11, the present data are compared with Nejat's Eq. (12) with the term $4(D_{he}/L_{C,B})^{1.396}$, since the values obtained by using Eqs. (9) and (10) scatter slightly as shown in Figs. 5 and 9. The values of Nejat's parameter $q^*_{C,N}$ for the flooding CHF predicted using Eq. (17) for C_w^2 is represented by a solid line in the figure because it does not quite present the scattering of the calculated values. The solid line shows excellent agreement with the present data. Figure 12 shows the comparison of the CHF predicted by Eq. (18) with the present CHF data. Equation (18) with Eq. (17) for C_w^2 predicts the present flooding CHF within an RMS error of 9.0 %. In practical application, since Equation (18) includes the unknown parameter $L_{C,B}$, for a given pressure, the axial heat flux distribution shape and geometry, the CHF value may be calculated by iteration using the relationship $q_Z = \frac{1}{Z - Z_{sat}} \int_{Zsat}^{Z} q(z)dz$, where q_Z is the average heat flux from Z_{sat} to location Z. However, the term $D_{he}/L_{C,B}$ in Eq. (18) may become the different functional form according to the axial heat flux shape condition. Hence, the further analytical studies for predicting the location of the flooding CHF are required.

5. Conclusions

The experimental study of water CHF under zero flow conditions were carried out in an annulus flow channel with uniformly and non-uniformly heated sections over a pressure range of 0.52 to 14.96 MPa. The present experimental data are compared with several existing flooding CHF expressions. The following conclusions can be drawn from this study:

(1) When Eq. (14), based on the Kutateladze flooding criterion, and Imura et al.'s correlation are used with Park et al.'s correlation for C_w^2, the parameter $q^*_{C,k}$ gives reasonable agreement with the present data. However, the discrepancy due to the effect of the heat flux distribution cannot be improved.

(2) The density term in Park et al.'s correlation for C_w^2 was corrected corresponding to the present condition and the correction term $(D_{he}/L_{C,B})^{1.396}$ was proposed in order to take into account the effect of the heat flux distribution on the CHF. Equation (18) based on the Wallis flooding equation with Eq. (17) for C_w^2 predicts the measured flooding CHF within the RMS error of 9.0 %.

Nomenclature

A_B	heated area of the boiling length, m^2
A_f	cross sectional flow area of a channel, m^2
B_o	Bond number, $D_{hy}(gDr/s)^{1/2}$
C_k	constant in the Kutateladze flooding criterion
C_w	constant in the Wallis flooding equation
D	tube inner diameter, m
D_{he}	heated equivalent diameter, m
D_{hy}	hydraulic equivalent diameter, m
D^*	dimensionless diameter, D_{hy}/l
d	heater rod diameter, m
g	gravitational acceleration, m/s^2
h_{lg}	latent heat of evaporation, kJ/kg
Dh_{sub}	subcooling enthalpy at the bottom end of the heated section, K
j	superficial velocity, m/s
j^*	dimensionless superficial velocity, $jr^{1/2}(gDDr)^{-1/2}$
K	Kutateladze number, $jr^{1/2}(gsDr)^{-1/4}$
$L_{C,B}$	length from the onset of saturated boiling to the location of CHF occurrence, m
L_B	boiling length in the heated section, m
L_h	heated length, m
L_Z	length from the bottom end of the heated section to location Z, m
m	constant in the Wallis equation and Kutateladze criterion for flooding

P pressure, MPa
DP differential pressure, kPa
$q(z)$ axial heat flux profile of the heater rod, kW/m^2
q_{ave} average heat flux over the heated section, kW/m^2
$q_{C,B}$ average critical heat flux over the boiling length, kW/m^2
$q_{C,ax}$ critical heat flux in the axial direction, kW/m^2
q_Z average heat flux from Z_{sat} to location Z, kw/m^2
$q^*_{C,k}$ dimensionless CHF parameter in Eqs. (10), (14) and (15) , $q_{C,B}/[h_{lg}(g s r_g^2 Dr)^{1/4}]$
$q^*_{C,N}$ dimensionless CHF parameter in Eq. (12), $q_{C,B}/[h_{lg} r_g (g D_{hy})^{1/2}]$
$q^*_{C,w}$ dimensionless CHF parameter in Eq. (9), $q_{C,B}/[h_{lg}(g D_{hy} r_g Dr)^{1/2}]$
DT_{sub} subcooling temperature at the bottom end of the heated section, K
Z distance from the bottom end of the heated section, m

Greek symbols

a average void fraction from the bottom end of the heated section to location Z
a average void fraction for the saturated condition at the bottom end of the heated section
l length scale of Taylor instability, $(s/gDr)^{1/2}$, m
r density, kg/m^3
Δr density difference of liquid and vapor phase, $r_l - r_g$, kg/m^3
σ surface tension, N/m
x dimensionless parameter in the flooding CHF equations, $[1+(r_g/r_l)^{1/4}]^{-2}$

Subscripts

C critical heat flux
B boiling length
g vapor phase
exp experiment
k Kutateladze's flooding criterion
l liquid phase
N Nejat's correlation
$Pred$ prediction
sat saturation condition
sub subcooled condition
w Wallis's flooding equation
Z location in the axial direction from the bottom end of the heated section

Acknowledgment

The authors would like to thank the Ministry of science and technology of Korea for their financial support of the Long-term Nuclear R & D Program.

References

1. Barnard, D. A., Dell, F. R. and Stinchcombe, R. A., (1974), Dryout at low mass velocities for an upward boiling flow refrigerant-113 in a vertical tube, UKEA, AERE-R 7726.
2. Mishima, K. and Nishihara, H., (1987), Effect of channel geometry on critical heat flux for low pressure water, *Int. J. Heat Mass Transfer*, **30**, 1169-1182.
3. EL-Genk, M. S., Haynes, S. J. and Kim, S. H., (1988), Experimental studies of critical heat flux for low flow of water in vertical annuli at near atmospheric pressure, *Int. J. Heat Mass Transfer*, **31**, 2291-2304.
4. Chang, S. H., Baek, W. P. and Bae, T. M., (1991), A study of critical heat flux for low flow of water

in vertical round tube under low pressure, *Nucl. Eng. Des.* **132**, 225-237.
5. Wallis, G. B., (1969), One-dimensional Two-phase flow, McGraw-Hill, 336-342.
6. Biasi, L., Cleriei, G. C., Garribba, S., Sala, R. and Tozzi, A., (1967), Studies on burnout, Part 3-A new correlation for round ducts and uniform heating and its comparison with world data, *Energ. Nucl.*, **14**, 530-537.
7. Groeneveld, D. C., Cheng, S. C. and Doan, T., (1986), 1986 AECL-UO critical heat flux look-up table, *Heat Transfer Engineering*, **7**, (1-2), 46-62.
8. Zuber, N., (1959), Hydrodynamic aspects of boiling heat transfer, USAEC Report, AECU-4439.
9. Griffith, P., Pearson, J. F. and Lepowski, R. J., (1977), Critical heat flux during a loss-of-coolant accident, *Nuclear Safety*, **18**, 298-305.
10. Chun, S. Y., Moon, S. K., Ahn, S. M., Yang, S. K. and Chung, M. K., (1998), Critical heat flux under zero flow conditions in vertical annulus, *Proceedings of the Korean Nuclear Society Autumn Meeting.*
11. Chun, S. Y., Ahn, S. M., Moon, S. K., S. M., Yang, S. K. and Chung, M. K., (1999), Critical heat flux under zero flow conditions in non-uniformly heated vertical annulus, *Proceedings of the Korean Nuclear Society Autumn Meeting.*
12. Chun, S. Y., Chung, H. J., Hong, S. D., Yang, S. K. and Chung, M. K., (2000), Critical heat flux in uniformly heated vertical annulus under a wide range of pressure – 0.57 to 15.0 MPa, *Journal of the Korean Nuclear Society*, **32**, 128-141.
13. Sakhuja, R. K., (1973), Flooding constraint in wickless heat pipes, ASME Paper 73-WA/HT-7.
14. Nejat, Z., (1981), Effect of density ratio on critical heat flux in closed end vertical tubes," *Int. J. Multiphase Flow*, **7**, 321-327.
15. Bankoff, S. G. and Lee, S. C., (1983), A critical review of the flooding literature, NUREG/CR-3060 R2, Northwest University, USNRC, 70-71.
16. Tien, C. L. and Chung, K. S., (1979), Entrainment limits in heat pipes, *AIAA Journal*, **17**, 643-646.
17. Imura, H., Sasaguchi, K., Kozai, H. and Numata, S., (1983), Critical heat flux in closed Two-phase thermosyphon, *Int. J. Heat Mass Transfer*, **26**, 1181-1188.
18. Park, C., Beak, W. P. and Chung, S. H., (1997), Countercurrent flooding limited critical heat flux in vertical channels at zero inlet flow, *Int.Comm. Heat and Mass Transfer*, **24**, 453-464.
19. Katto, Y. and Hirao, T., (1991), Critical heat flux of counter-flow boiling in a uniformly heated vertical tube with a closed bottom, *Int. J. Heat and Mass Transfer*, **34**, 993-1001.

Table 1. Ranges of the present experimental data and applicable ranges of the Park et al. [18] correlation (Eq. (16)) for C_w^2

	Present work	Park et al. [18]
Test section Geometry	annulus	Round tubes, annuli and rectangular channels
Fluid	water	water and Freon 113
Hydraulic equivalent Diameter (D_{hy})	9.86 mm	4.8~17.2 mm
Length to diameter ratio (L_B /D_{he})	48.0~59.8	8.1~120.0
Liquid to vapor ratio (r_l/r_g)	6.2~335.6	200~1600
Bond number (B_o)	4.25~10.0	1.79~17.3

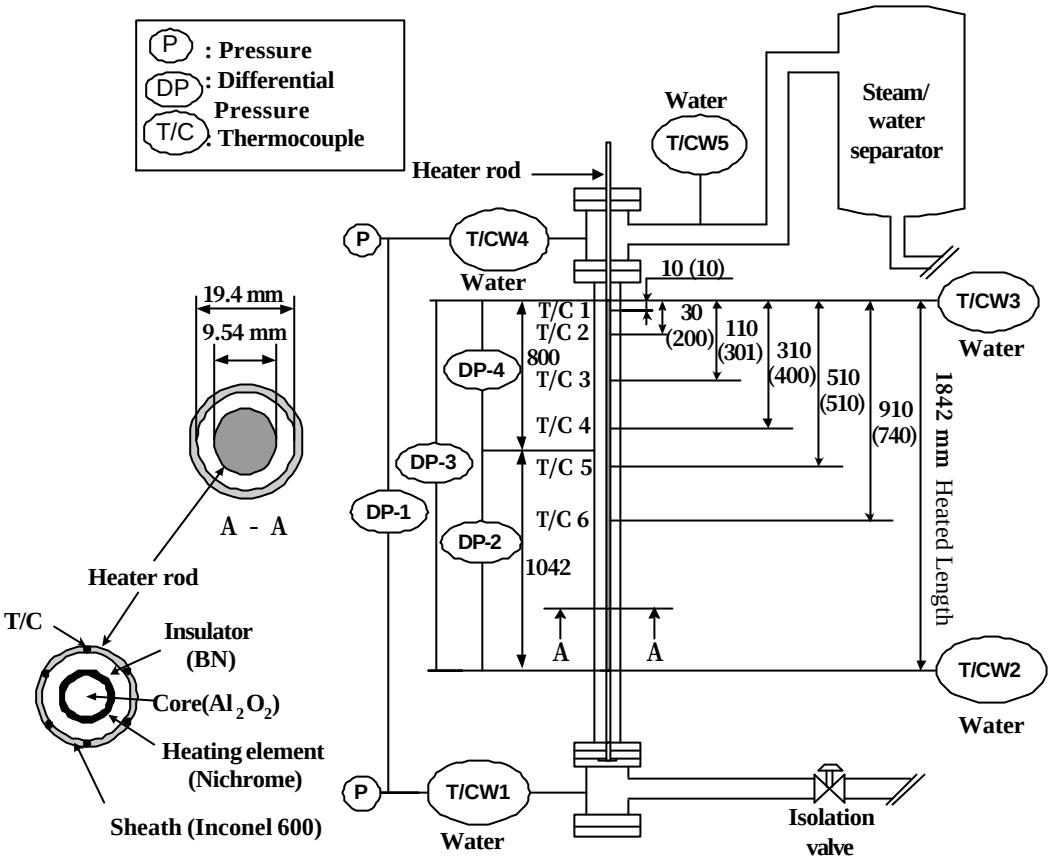

Fig. 1. Test section geometry and the locations of measuring sensors – ( ) denote the thermocouple locations of the heater rod with non-uniform heat flux distribution

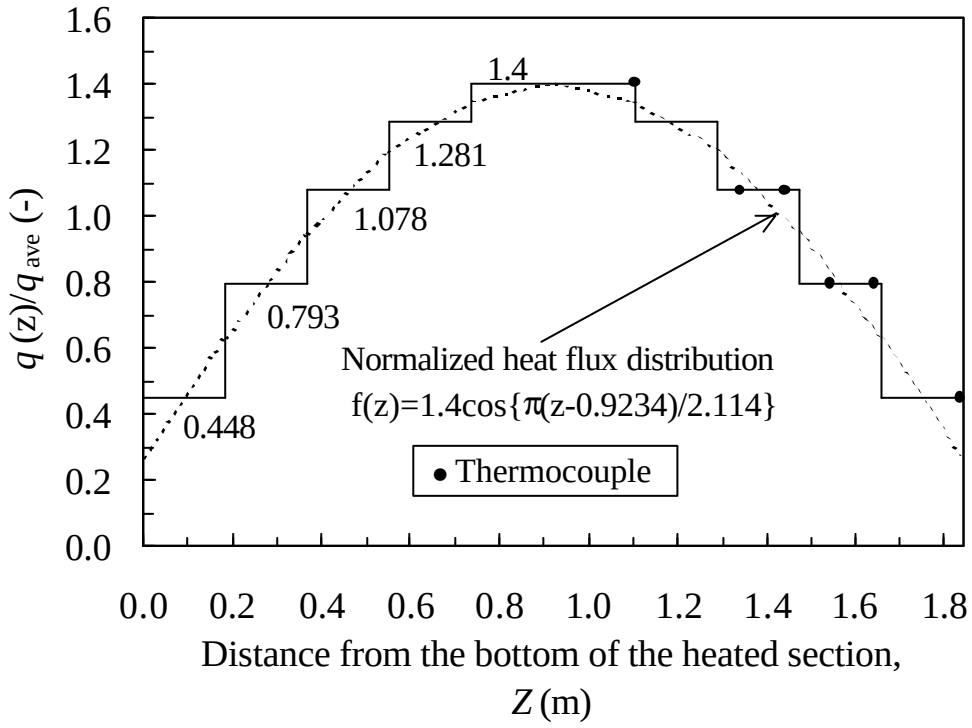

Fig. 2. Heat flux distribution of the non-uniform heater rod

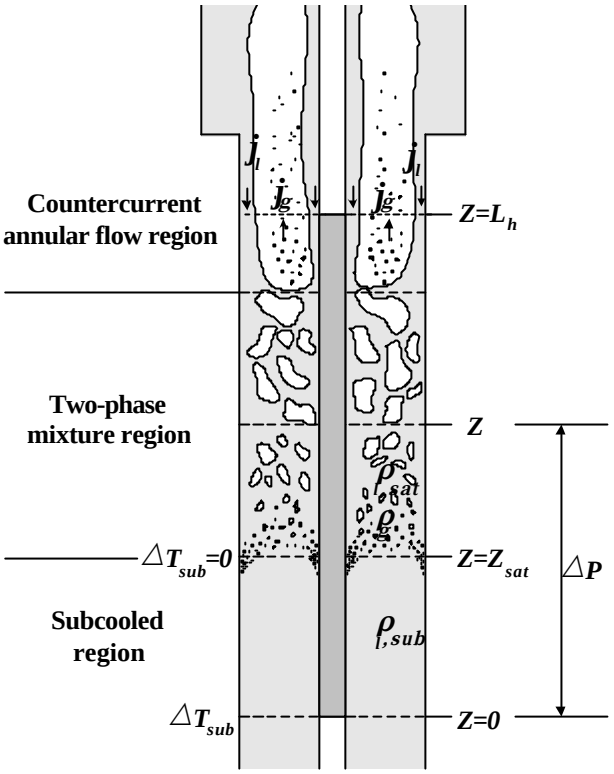

Fig. 3. Physical model of the present boiling system

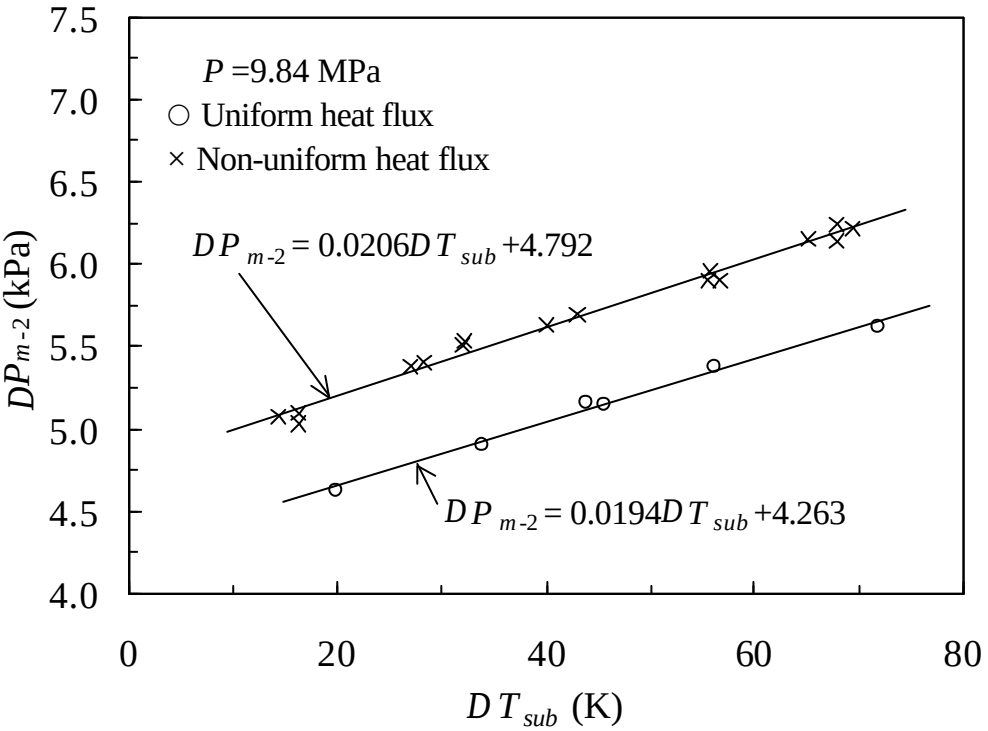

Fig. 4. Relationship of the pressure drop ($DP_{m\text{-}2}$) and the subcooling temperature at the bottom end of the heated section

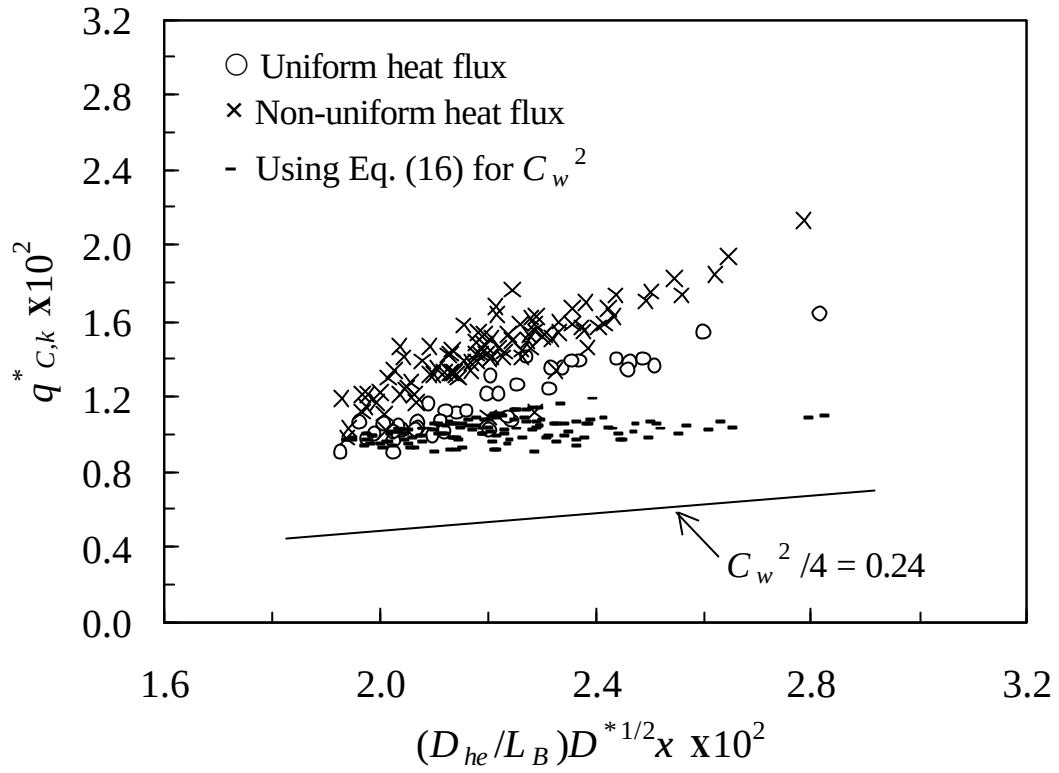

Fig. 5. Comparison of the present data with Mishima and Nishihara's equation (Eq. (10))

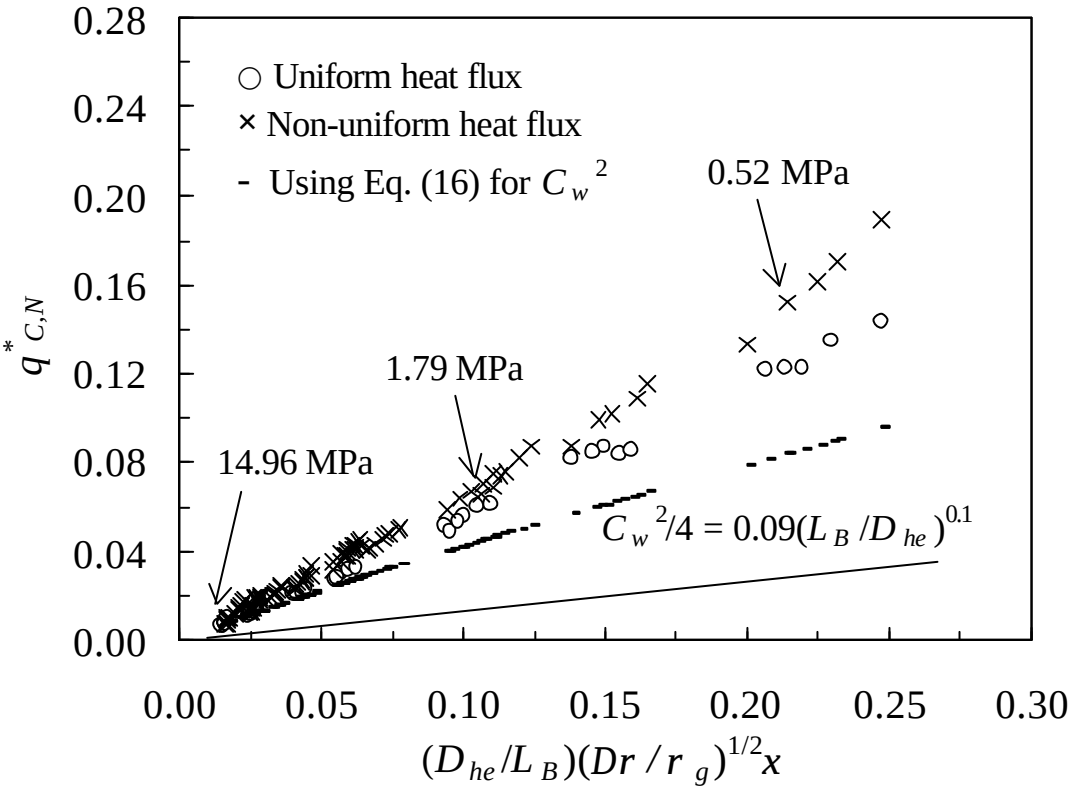

Fig. 6. Comparison of the present data with Nejat's equation (Eq. (12))

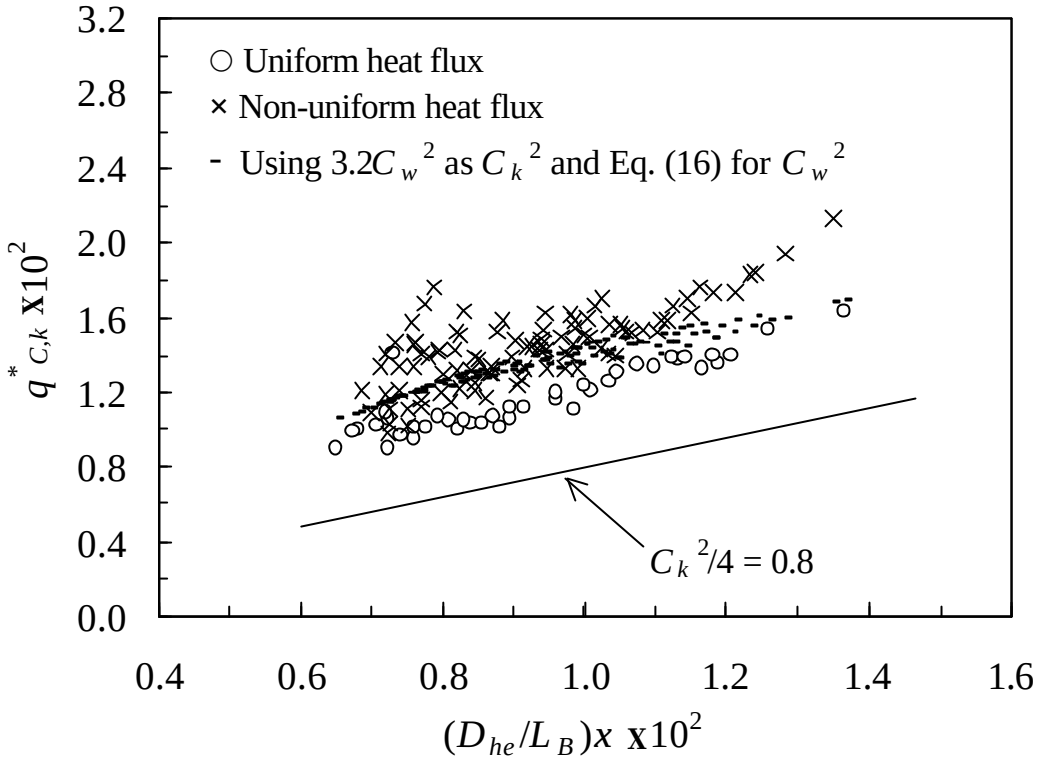

Fig. 7. Comparison of the present data with Tien and Chung's equation (Eq. (14))

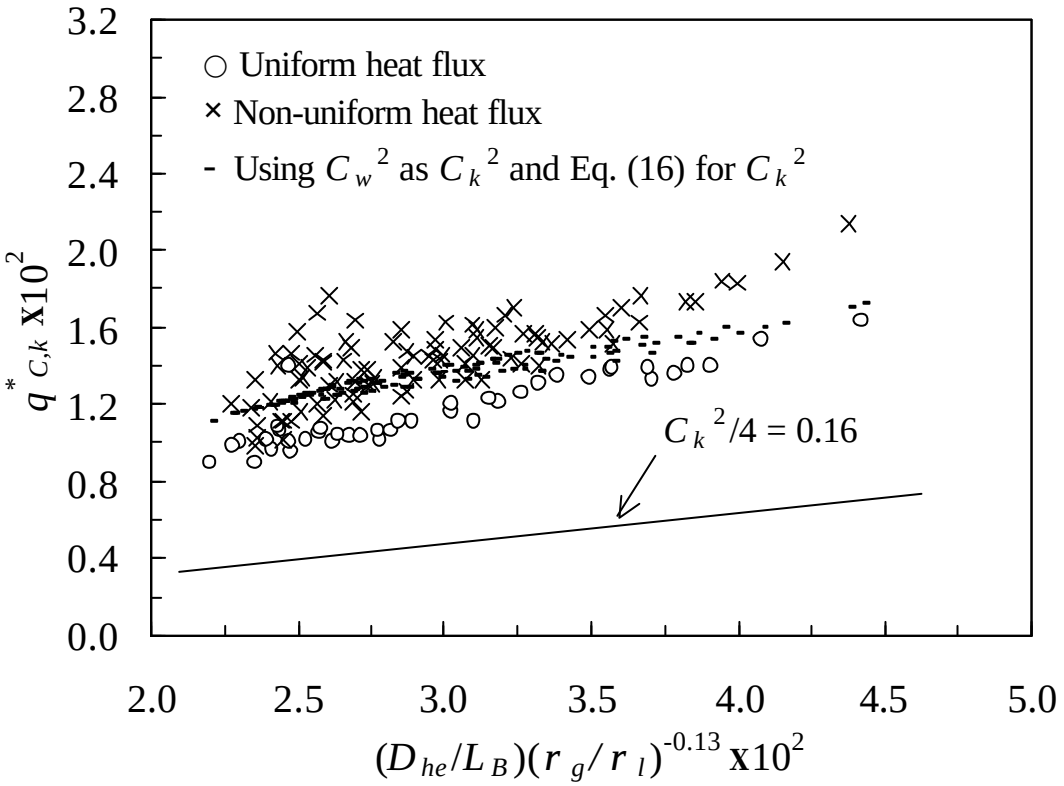

Fig. 8. Comparison of the present data with Imura et al.'s correlation (Eq. (15))

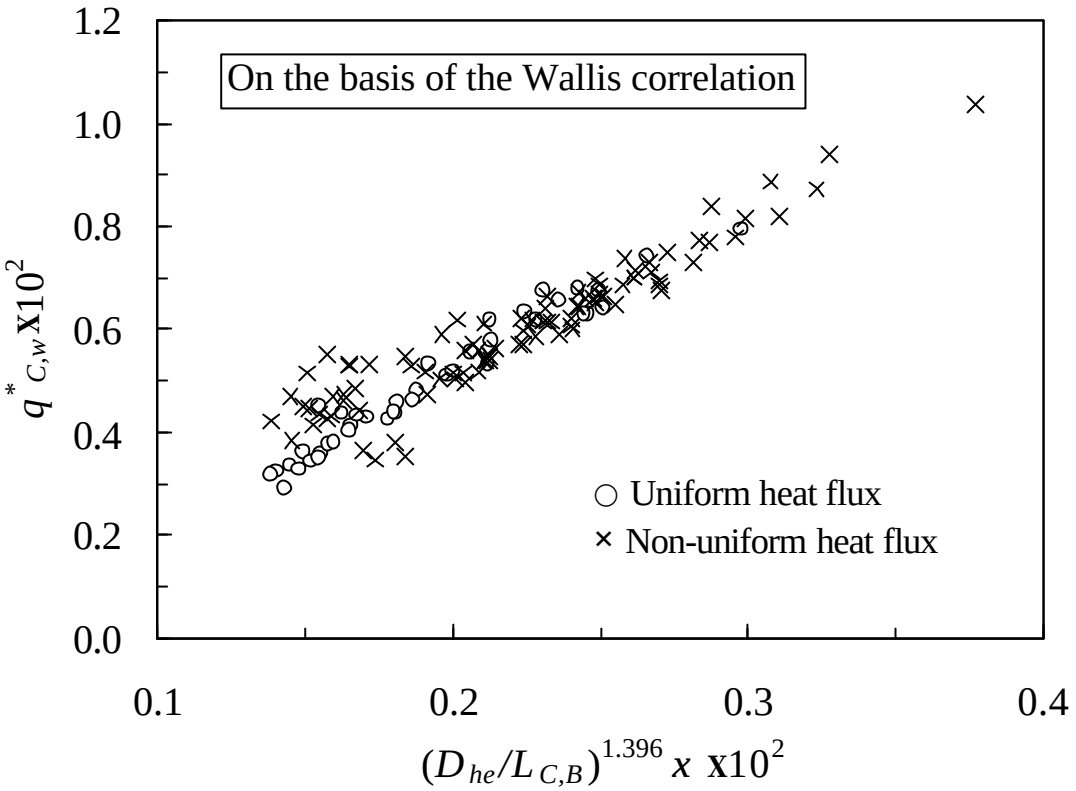

Fig. 9. Comparison of the present data with the modified Wallis flooding CHF correlation

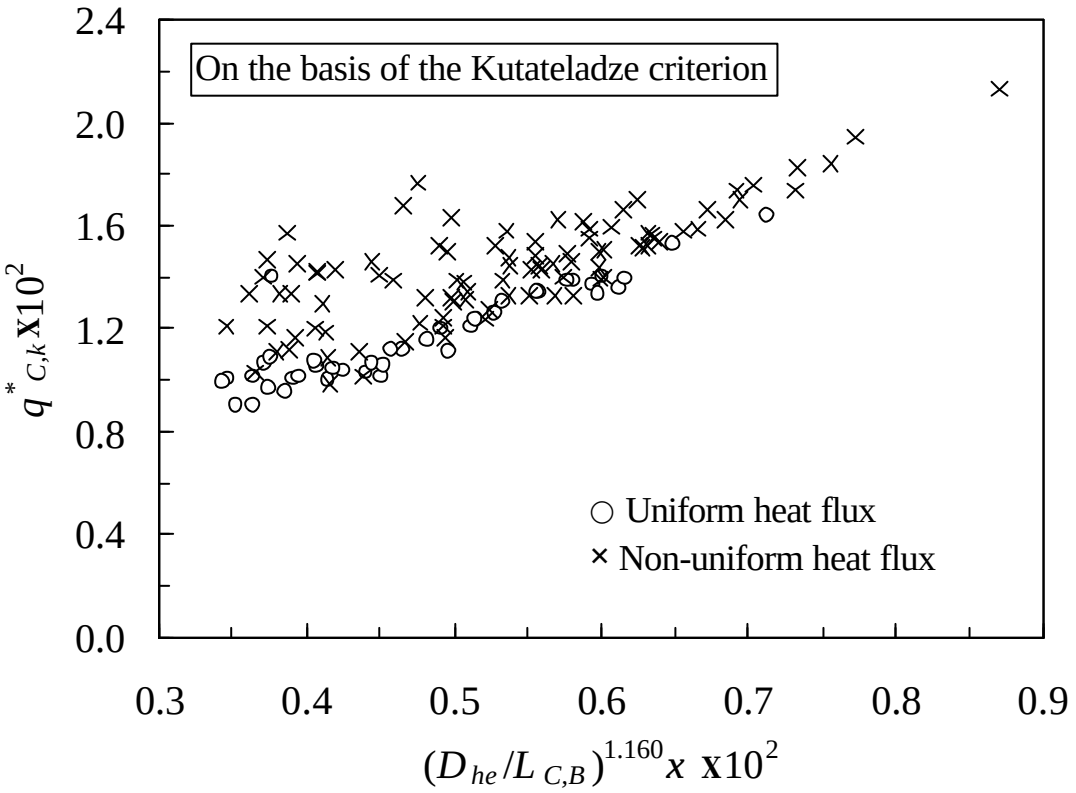

Fig. 10. Comparison of the present data with the modified Kutateladze flooding CHF correlation

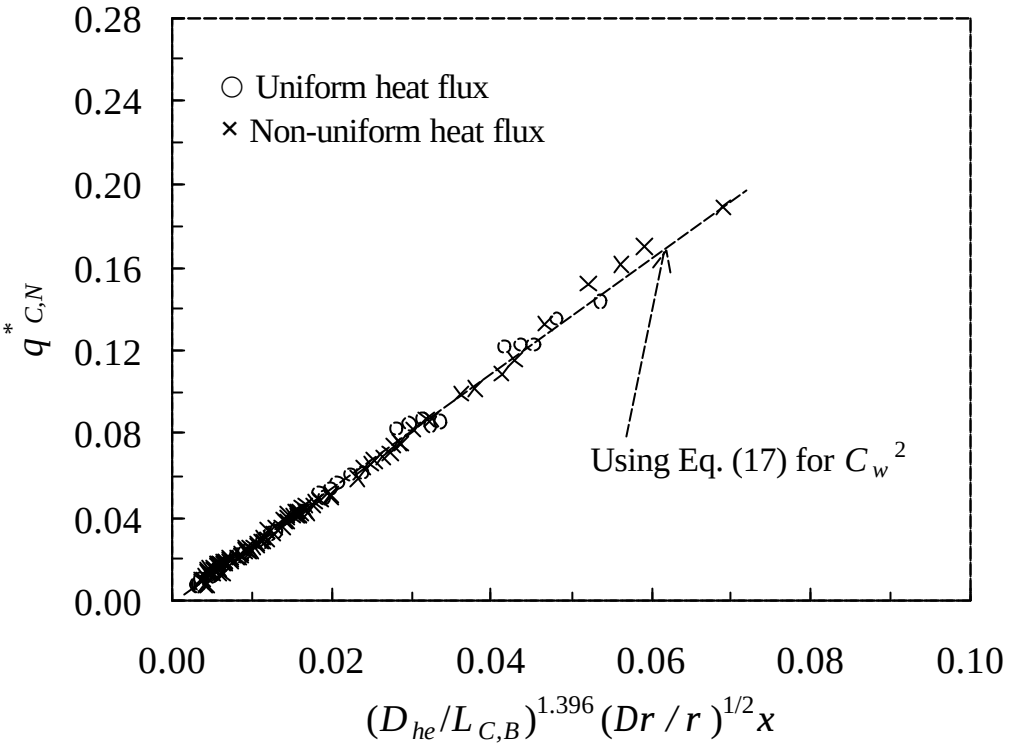

Fig. 11. Comparison of the present data with the modified Nejat equation

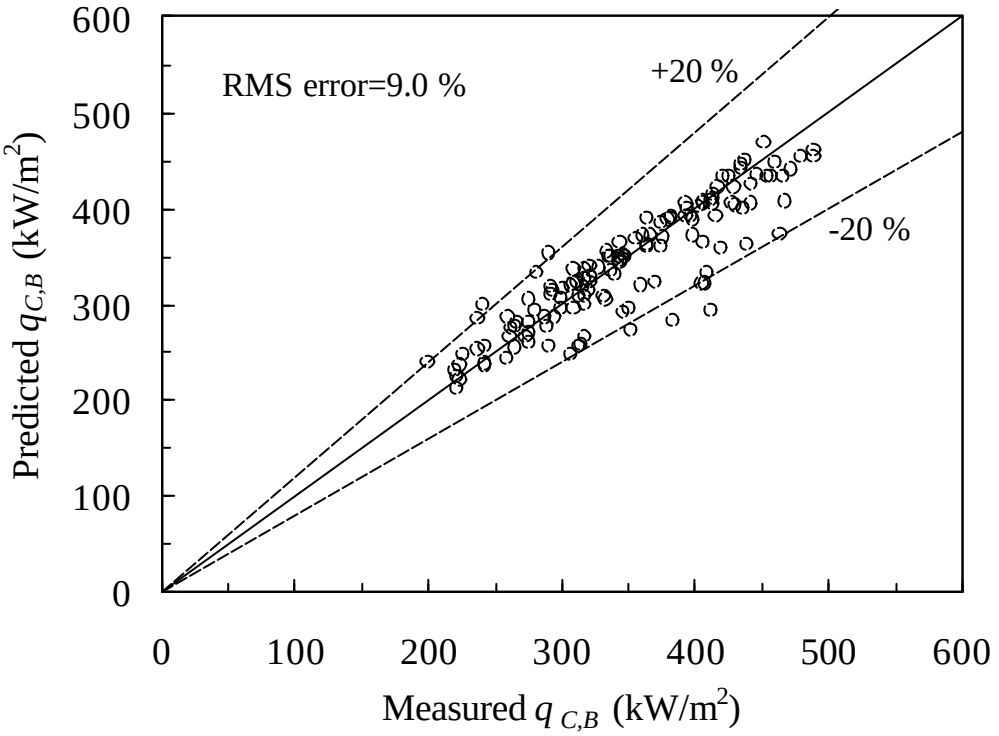

Fig. 12. Comparison of the present CHF with the CHF predicted by Eq. (18) with Eq. (17) for $C_w{}^2$,

RMS error $= \sqrt{\frac{1}{N}\sum_{i=1}^{N}\left(\frac{q_{C,B,pred} - q_{C,B,\exp}}{q_{C,B,\exp}}\right)^2}$, where N is the total number of data.

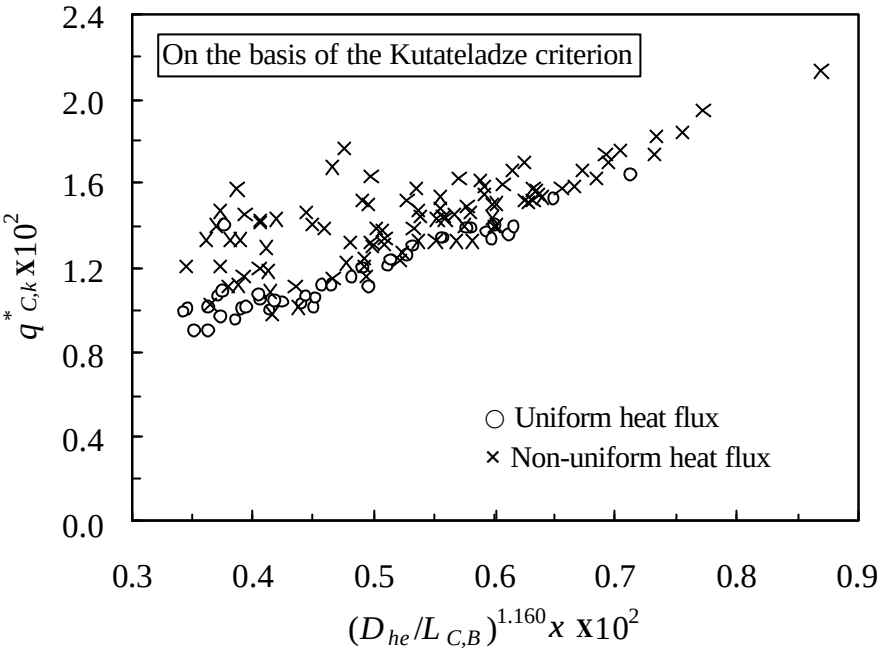
On the basis of the Kutateladze criterion
○ Uniform heat flux
× Non-uniform heat flux
$q^*_{C,k}$ X10^2
$(D_{he}/L_{C,B})^{1.160}x$ X10^2
2.4
2.0
1.6
1.2
0.8
0.4
0.0
0.3
0.4
0.5
0.6
0.7
0.8
0.9